

Journal of Physical Chemistry and Functional Materials (JPCFM)

journal homepage: <http://dergipark.gov.tr/jphcfum>



Received: November 12

Accepted: 21 November 2018

Research Article

Investigation of Thermal properties, Chemical Analysis and Biocompatibility of High

Mediha K k^{1*}, Fethi Dağdelen¹, Gonca Ateş¹, Z. Deniz  rak²

¹Firat University, Science Faculty, Department of Physics, Elazığ, TURKEY

²Inonu University, Vocational School of Health Service, Malatya, TURKEY

*Corresponding Author: msoglu@firat.edu.tr

Abstract

In recent years, studies have been conducted on the biocompatibility of NiTi-based shape-memory alloys, which are used in medical application. In this study, the oxidation process of Ni₄₈Ti₅₁Mn alloy produced with Arc Melter Method with the Thermogravimetric Analysis Device (TG/DTA) was performed to improve biocompatibility for three different oxidation temperatures (600-700-800°C). The oxidation rate of the alloy that was exposed to isothermal oxidation was calculated. With the increase in the oxidation temperature, the alloys were oxidized faster. The change of the oxidation on the Shape-Memory Effect (SME) of the NiTiMn alloy was determined by Differential Scanning Calorimetry (DSC), and it was observed that the SME did not disappear. The changes occurring on the surface and on the crystal structure of the alloy were determined by SEM-EDX and X-ray analyses. It was determined with chemical analysis (EDX) that a TiO₂ layer was formed on the alloy. The fact that the TiO₂ layer increased with the increase in the oxidation temperature was supported with x-ray measurement results. In this way, it was concluded that there was a protective oxide layer on the surface of the alloy. ICP-MS measurements were done to determine penetration of Ni, Ti and Mn element of oxides alloys in to Ringer solution.

Key Words: NiTi based alloy, oxidation, phases, thermogravimetric analysis, Biocompatibility.

1. Introduction

Medical implants have had an important value in medical world in recent years. They are used in more than one hundred million people. On the other hand, prosthesis studies that were worth over 50 million dollars were conducted in institutes and studies on bioengineering or biomedical engineering were conducted in more than 150 universities throughout the world. Many medical devices are made from metallic, ceramic, polymeric and composite biomaterials. Among these industrial materials, NiTi shape-memory alloys are used in orthopedics, surgery, dentistry and in more recent years, in cardiovascular devices [1-3].

In recent studies, the biocompatibility of shape-memory alloys has been examined in *in vitro* (artificial body medium) and *in vivo* medium (natural body medium). The purpose in these studies was determining the reaction of the body to these alloys [3-6]. NiTi alloys show toxic properties in the body because of the nickel element in them. To prevent Ni element from being harmful for the body by bonding with body fluids or blood, it has to be converted into passive mode from active mode [7-9]. For this purpose, the active nickel elements in the NiTi alloy are mostly passivized with laser oxidation, ion implantation and thermal processes. The Ti element in NiTi merges with the oxygen applied to the alloy, forms the TiO₂ compound, and prevents the Ni element from passing to external surface that is in contact with the body with a barrier-like mechanism [2]. For this reason, the oxidation properties of NiTi and NiTiX alloys must be examined in detail. Examining the oxidation properties of shape-memory alloys with TG/DTA is a new method. The advantage of this method is being able to determine the time spent for the oxygen saturation temperature. In addition, it is also possible to determine the oxidation constant, which is the indicator of oxidation rate, with this method.

In the context of the purpose of the study, oxidation will be applied to alloys with TG/DTA device, which is considered as a method to increase the biocompatibility of NiTiMn shape-memory alloys (which transform at body temperature). This process will be applied at high temperatures and the oxidation constant, which is the indicator of the oxidation rate of the alloy, will be determined. Then, the oxide phases will be determined with the chemical analysis and X-ray method. In this way, the purpose is to determine the advantages and disadvantages of oxidation of the NiTiMn alloys that transform at body temperature as implant.

2. Experimental Procedure

The Ni₄₈Ti₅₁Mn (atomic percentage) shape-memory alloy was used for the experiments. This alloy was obtained by melting in the Arc Melter furnace. The melting process was repeated several times and primary homogenization was applied to the alloy. The secondary homogenization was performed by keeping the alloys at 1050°C for 24 hours. The martensite transformation temperature of the alloy was measured by Perkin Elmer Sapphire Differential Scanning Calorimeter at nitrogen atmosphere with 20°C/min heating rate, and it was determined that the alloy was transformed near the body temperature (37°C). 600, 700, 800°C isothermal oxidation process was applied to the alloys that were cut as smooth pieces with the TG/DTA (Perkin Elmer Pyris Thermogravimetry / Differential Thermal Analysis) Device for 1 hour. Then, it was checked whether there were any changes at the transformation temperatures of these alloys with DSC. The crystal structure, surface morphology analysis of the oxidized alloys and thickness of oxide layers were performed with X-ray (XRD) (Rigaku RadB-DMAX II) and SEM-EDX measurement (JEOL JSM 7001F). Vickers microhardness measurement of oxidized alloys was made using Emco Test DuraScan microhardness testing machine.

Ni₄₈Ti₅₁Mn (in atomic percentage) shape memory alloys show transformation at body temperature, because of this results, biocompatibility of this alloy were determined by Perkin Elmer ICP-MS (Inductively Coupled Plasma – Mass Spectrometer) device. The 100 mg parts of Non-oxide and oxide alloys put into 10 ml ringer solution for 14 days at 37 °C.

3. Results and Discussions

In order to apply oxygen to NiTiMn alloy samples that were prepared for oxidation at fixed temperature, the Perkin Elmer Pyris-TG/DTA device was used. The samples were placed in the TG/DTA furnace, and were heated at pure nitrogen gas atmosphere with 50°C/min heating rate to reach the desired oxygen application temperature. The reason of heating the alloy in the nitrogen gas atmosphere is to prevent that it is exposed to the oxygen in the air. Heat treatment is important NiTi shape memory alloys to improve work hardening extremely rapid during cold-deformation. Generally, heat treatment temperatures of NiTi shape memory alloys are between 500 and 800 °C. High temperature in atmosphere containing oxygen will result in the oxidation of the alloys [10-12]. Therefore, 600, 700 and 800°C were chosen as the oxidation temperature. The alloy, which was brought to oxidation temperature in TGA furnace, was kept at this temperature for 1 hour. Under fixed temperature, oxygen gas was given to the alloy with 100 ml/min flow rate, and it was oxidized. Depending on the mass gain, the isothermal oxidation constant (K_p) was calculated by making use of the following formula:

$$\left(\frac{\Delta W}{A}\right)^n = K_p t \quad (1)$$

In general terms, the increase of the mass of a metal as a result of oxidation can be linear increase or parabolic. In order to calculate linear isothermal oxidation Constant, n=1 is taken; in order to calculate the parabolic isothermal oxidation constant, n=2 is taken. As seen from Fig. 1, the curve of the mass increase is parabolic, so n=2 was taken. The slope of the $(\Delta W/A)^2$ against time (t) gives us the oxidation constant (K_p) [13].

In Figure 1, the mass gain curves that occur with the oxidation in NiTiMn are given. As the oxidation temperature increases, the mass gain of the alloy based on the oxygen also increases. The oxidation constant values that were calculated according to the equation increased in direct proportion with the increase in oxidation. The reason for this is the activation of the elements that have the slope of being oxidized in the alloy with the temperature and binding with oxygen. Our results are in accordance with the literature. Xu et al., calculated the oxidation constants of NiTi alloy, which included 50.8% Titanium in atomic terms, in air atmosphere and in argon gas atmosphere for 600, 700, 800°C with TG/DTA device in 20 h isothermal medium. The oxidation constant values are as follows: For 600°C, 8.3×10^{-9} - 2.78×10^{-9} mg²/mm⁴s⁻¹; for 700°C, 3.1×10^{-8} - 2.22×10^{-8} mg²/mm⁴s⁻¹; and for 800°C, 1.0×10^{-6} - 0.6×10^{-6} mg²/mm⁴s⁻¹. The values reported by Xu et al. are close to the ones found by us as given in Table 1 [14]. One of the reasons of the difference is the chemical ratio of the alloy (there is manganese in our alloy), and the other reason is the oxidation performed in oxygen atmosphere. Firstov et al. and Hansen et al. conducted a study and performed oxidation process in which they applied non-isothermal

oxidation process to NiTi alloys at various rates with TG/DTA device. In this reason, they could not calculate oxidation constant. [15.16].

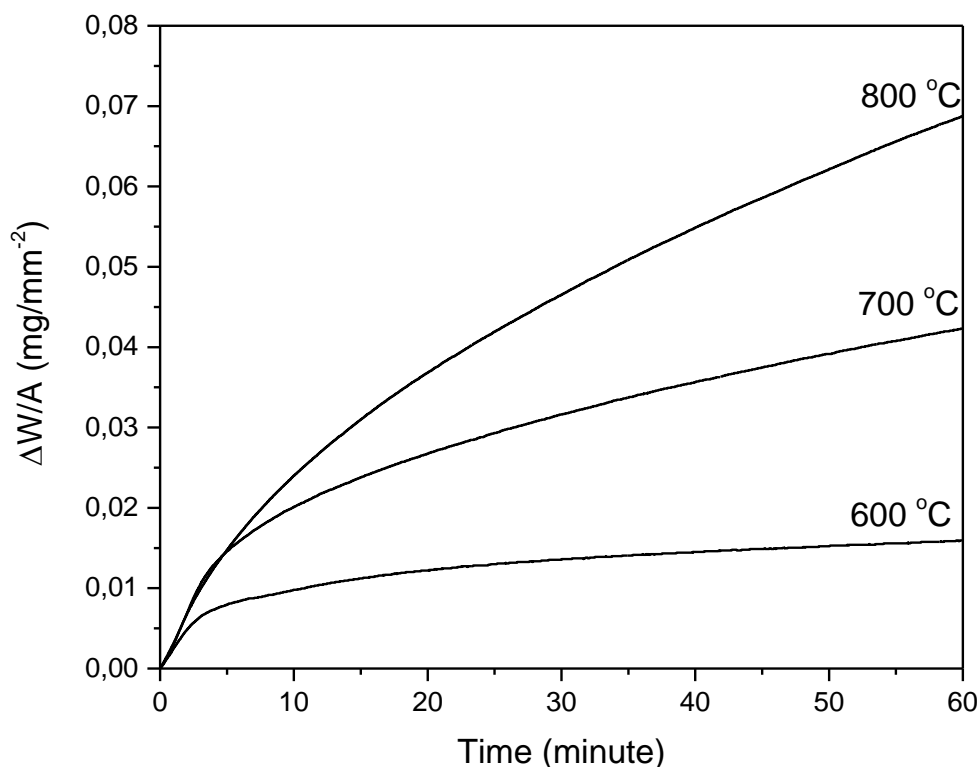


Figure 1 Mass gain of Ni₄₈Ti₄₉Mn shape-memory alloys at different oxidation temperatures

Table 1. The oxidation constant values of the oxidized Ni₄₈Ti₄₉Mn shape-memory alloys (R²:correlation coefficient)

Oxidation Temperature (°C)	Oxidation Constant (Kp) (mg ² /mm ⁴ s ⁻¹)	R ²
600	5.42x10 ⁻⁸	0.93
700	4.69x10 ⁻⁷	0.96
800	1.37x10 ⁻⁶	0.99

It was decided whether there was a change in the transformation temperature of the Ni₄₈Ti₄₉Mn after oxidation by using the DSC measurements. After 600, 700 and 800°C oxidation, the austenite start-final (As-Af), martensite start-final temperature (Ms-Mf) values of the alloy are given in Figure 2 and Table 2. According to DSC results, it is clearly seen that the shape-memory effect of this alloy still

continues even after oxidation. However, changes occurred in transformation curves and temperatures with the increase in the oxidation temperature. In order to see the comparison clearly, the transformation temperature results of the non-oxidized alloy are added to Table 2. In this context, R phase decreased at 800°C in such a level that could not be detected in oxidation. The transformation temperature range increased with the oxidation temperature in general sense. The alloy with the austenite-final temperature that is closest to the body temperature is the alloy that was processed with oxidation at 700°C. The results we have found are in accordance with the literature Sadrnezhad and his colleagues studied the biocompatibility of the porous NiTi shape memory alloy. In their study, they found an as temperature value of 27 °C and a Ms transformation temperature of 57 °C [17]. In another study, Huafang Li et al. produced a NiTiW shape memory alloy and studied at the in vitro biocompatibility of this alloy. They measured transformation temperatures of alloy by DSC and they found to as value is 332 K (59 °C) and Ms value is 337 K (64 °C) [18].

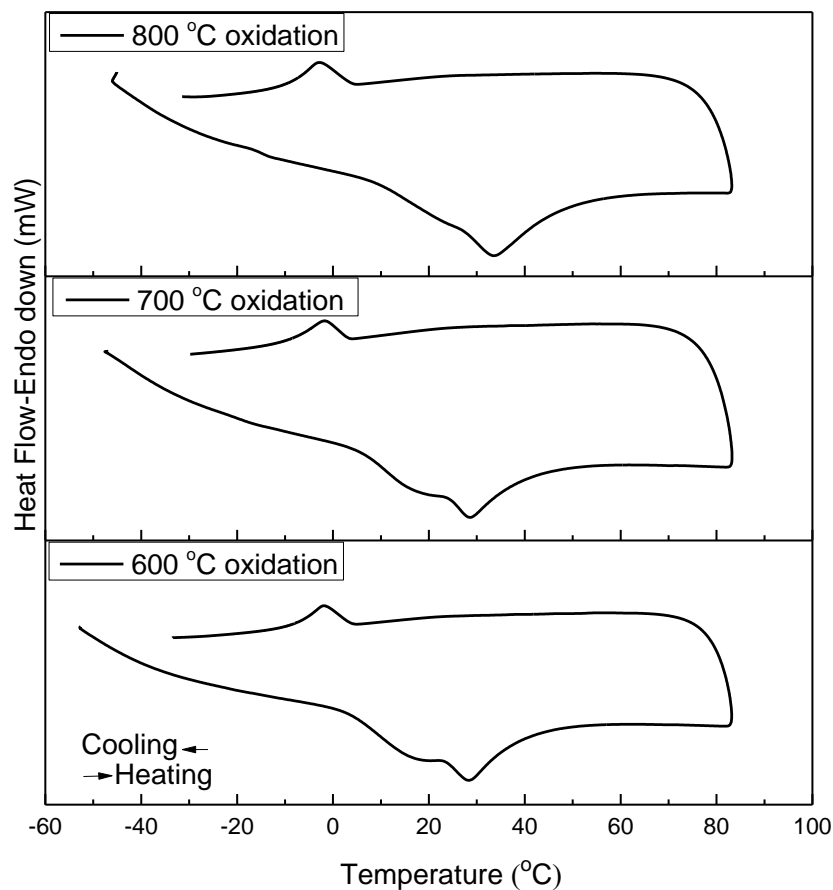


Figure 2 The DSC curves that give the transformation temperature of the Ni₄₈Ti₅₁Mn shape-memory alloys exposed to oxidation

Table 2. The changes that occur at the transformation temperature of the Ni₄₈Ti₅₁Mn alloys exposed to oxidation

Oxidation Temp. (°C)	Rs (°C)	As (°C)	Af (°C)	Ms (°C)	Mf (°C)
Non-oxide	0.3	17.6	34.6	4.4	-5.6
600	3.6	18.2	49.4	3.9	-8.8
700	6.9	18.1	46.4	3.3	-12.7
800	---	7.7	65.1	4.0	-11.5

In Figure 3a-c, the Scanning Electron Microscope (SEM) images of the Ni₄₈Ti₅₁Mn alloys exposed to oxygen for 1 hour at 600, 700 and 800°C taken at X15000 magnification are given. The grains of the alloy that is oxidized at 600°C and the Nano rods on the grains are clearly visible. When the chemical content of the Nano rods with EDX is considered, it is possible to claim that Nickel rate is 2.52%; Titanium rate is 26.38%; manganese rate is 0.84%, and oxygen rate is 70.27% in atomic percentage. Based on these results, it is possible to claim that there are Ni and Mn elements at a very low level with the TiO₂ oxide phase on the surface of the NiTiMn alloy. According to the general EDX results taken from the whole surface of the alloy, all the element ratios, the values at nano rod are almost the same. According to this result, there is TiO₂ oxide phase, nickel and manganese element at a very low rate on the surface of the alloy. With 700°C oxidation rate, it is seen that the grain size of the alloy increased, and nano rods disappeared. According to the general EDX results, nickel rate is 3.98%, titanium rate is 21.11%, manganese rate is 1.85%, and oxygen rate is 73.06% in atomic percentage. When these results are compared with the alloy that is oxidized at 600°C, it is seen that nickel increased and titanium decreased. Again, TiO₂ oxide phase, nickel and manganese elements at very low levels were detected on the surface. Nano rods are not seen after oxidation at 800°C, and a serious increase is seen in the grain size. This result is in agreement with the literature. Firstov et al. also reported similar results [15]. The increase observed in the grain size depending on the oxidation temperature stems from the expansion of the alloys. The expansion with temperature brings with it the expansion of the grain size. This result is an agreement with the previous study. In the study, oxidation was applied at 500, 600, 700, 800, 900°C to NiMnGa alloy, and a serious increase was observed in the grain size after oxidation [19]. According to the general EDX results received from the surface of the alloy oxidized at 800°C; nickel rate is 3.23%, titanium rate is 26.8%, manganese rate is 2.57% and oxygen rate is 67.40% in atomic percentage. These results are in agreement with the other oxidation temperatures. However, while there is an increase in titanium and manganese rate, there is a decrease in oxygen rate. In addition, the titanium rate (in atomic) is around 90%. The oxide layer thickness of the alloy was determined by SEM-EDX analysis as a roughly. The cross-section images can be seen in Figure 3d-f. The oxide layer thickness of the alloys is almost 8.19 μm, 10.80 μm and 14.30 μm, respectively. The thickness of the oxide layer increased with increasing oxidation temperature. Shima Hadad and colleagues found the thickness of the oxide layer of the anodized NiTi alloy to be 2 μm [20]. Compared to our study, it can be said that oxidation by temperature produces a thicker oxide layer than anodized.

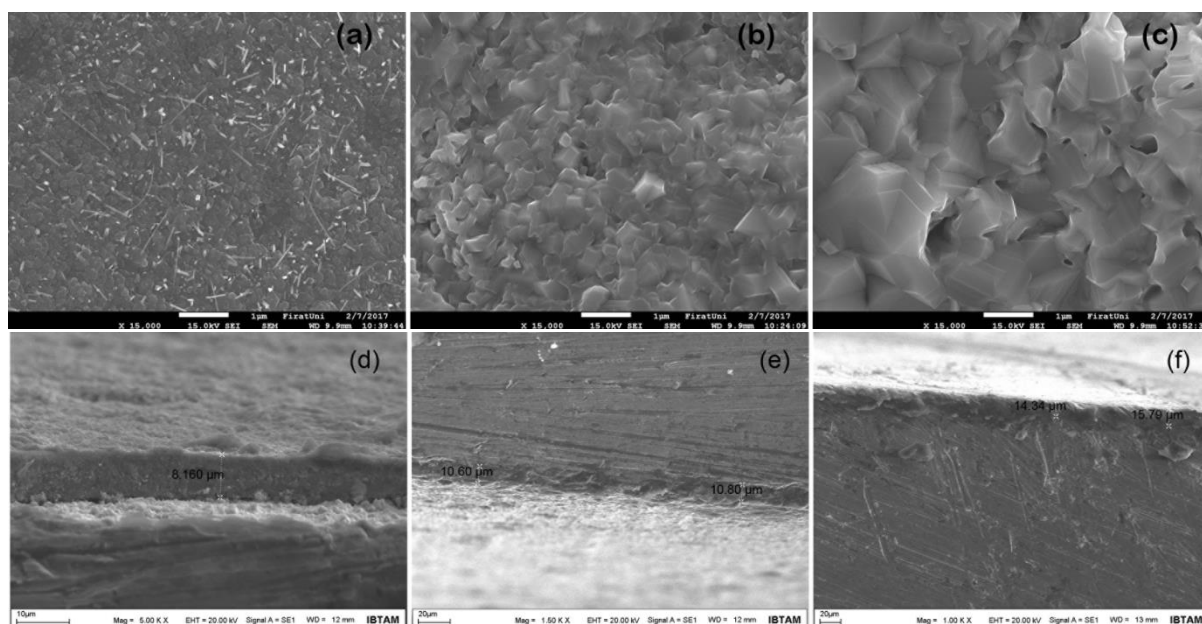


Figure 3 SEM images of oxidized $\text{Ni}_{48}\text{Ti}_{51}\text{Mn}$ shape-memory alloys a) 600°C oxidation temperature b) 700°C oxidation temperature c) 800°C oxidation temperature (one hour) and cross section images of oxidized $\text{Ni}_{48}\text{Ti}_{51}\text{Mn}$ shape-memory alloys d) 600°C oxidation temperature e) 700°C oxidation temperature f) 800°C oxidation temperature

We may obtain certain data on the oxide phases that occur on the surface of the NiTiMn alloy after oxidation from the X-ray measurement results. The XRD diffractograms taken at 25-80° range at room temperature of the alloys oxidized at 600, 700 and 800°C are given in Figure 4. The indexing of the X-rays was made according to the JCPDS cards and literature [21-23]. (JCPDS card no:65-4572, 65-5746, 18-0898,65-0192, 02-0567, 01-1292)

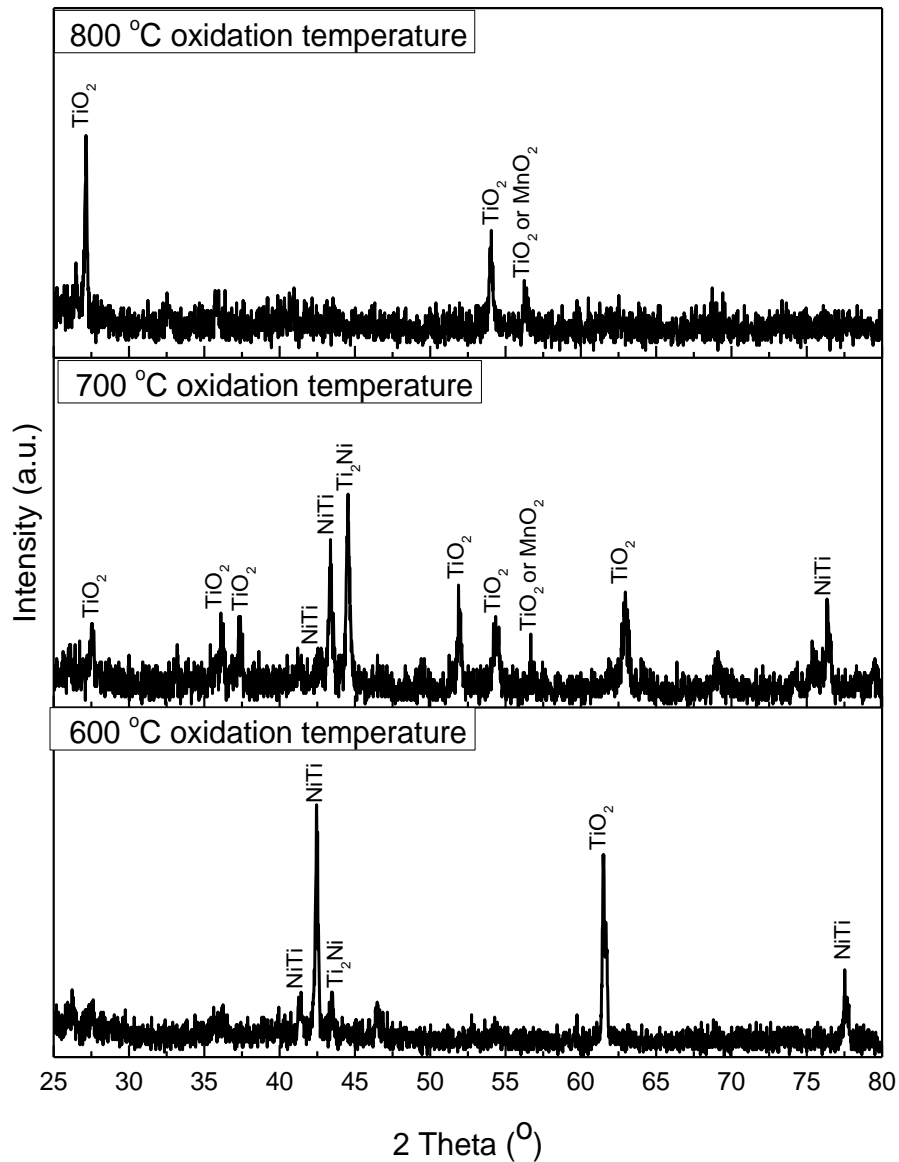


Figure 4 X-ray diffractograms of the $\text{Ni}_{48}\text{Ti}_{51}\text{Mn}$ shape memory alloys exposed to oxidation

When Figure 4 is observed, it is seen that the number of the peaks of oxide phase increased with the increase at oxidation temperature, and the intensity of the peaks of the (NiTi , Ti_2Ni) phases of the main phase decreased. It was seen in the X-ray diffractogram of the alloy oxidized at 800°C that the peaks of the oxide phase were dominant, and the peaks of the main phase were so low that they were almost invisible. This result is in agreement with the literature. Chu et al. applied Fenton's oxidation to NiTi alloy, and reported as a result of the X-ray measurements that there was TiO_2 phase on the surface, and Ni and metallic phases of Ni on the internal part [22-24]. The reason why there was oxide phase on the surface of the alloy may be explained as follows; when the combination value of the oxygen with

nickel and titanium element is examined, it is possible to say that titanium is easily oxidized, and nickel is oxidized with difficulty [25-26]. In addition, MnO₂ phase was detected at a very low level in the alloy oxidized at 800°C.

Mikro hardness measurements of oxidized alloys were made with load of 100 gf. The average microhardness values results are as follows: Hardness value for an oxidizing alloy at 600 °C is 362 HV, hardness value for an oxidizing alloy at 700 °C is 546 HV, and for an oxidizing alloy at 800 °C is 906 HV. The hardness values of alloys are increased by the oxidation temperature. The reason of the increasing hardness values by the high oxidation temperature can be explained as increase of the TiO layer on the alloys' surface. Because the hardness value of the TiO₂ compound is 1130 HV [27]. The cracks were not observed in the oxide layer that formed on the alloys after the hardness measurements.

Table 3. The penetration rate of NiTiMn alloys element for non-oxide and oxide alloys for 14 days. (Ni, Ti and Mn element amount in pure ringer solution were given for comparing)

	Ti (ppm)	Mn(ppm)	Ni (ppm)
Pure Ringer Solution	0.249	0.273	0.271
For non-oxide Alloy	0.318	0.793	239.50
For Oxide Alloys			
at 600 °C	152.4	191.5	2.76
at 700 °C	542.2	56.9	1.98
at 800 °C	213.0	4.0	1.8

According to ICP-MS measurement, the amount of Ni, Ti and Mn element in ringer solution were given in Table 3. Ni element amount is highest for non-oxide alloy, by oxidation the amount of Ni element is decreasing and others element (Ti and Mn) values are increasing into ringer solution. It can be said that, oxidation is good procedure to eliminate Ni element and the oxidation is important application to build barrier for Ni element.

4. Conclusions

The changes that occurred on the NiTiMn alloy exposed to isothermal oxidation with thermogravimetric analysis method are summarized as follows.

- The oxidation rate increased as the oxidation temperature of the NiTiMn alloys increased. The increase in the activity of oxygen means that it forms oxide phases.
- No serious increases were observed at transformation temperatures of the alloy as a result of the oxidation. The alloy was transformed at a temperature that is close to body temperature. The severity of the peak of the R phase in the alloy that was oxidized at 800°C decreased at a serious level.
- As a result of the SEM-EDX analysis, TiO₂ phase was observed frequently on the surface of the alloy. At 800°C, which is the highest oxidation temperature, it was determined with the X-ray measurement results that there is an increase in the titanium oxide phase amount. In addition,

according to the SEM images an increase was observed in crystal size with the increasing oxidation temperature. In the alloy that was oxidized at 600°C, oxide nano rods were detected, which is different from the other alloys.

- The thickness of TiO₂ layers and microhardness values were increased with rising oxidation temperature.
- In NiTiMn alloy, the formation of oxide TiO₂ and Ti and Mn₂O phase in between created a barrier to nickel on the surface of the alloy. This oxidation shows that it is important to increase the biocompatibility of the alloy.

ICP-MS results show that oxidation built oxide barrier especially TiO₂ on NiTiMn alloys. By oxidation, amount of Ni element decreased and Ti and Mn elements amounts increased in ring solution.

Acknowledgements

This work was supported by Management Unit of Scientific Research projects of Firat University (FUBAP) (Project Number: FF.16.32).

5. References

- [1]. S.K. Sadrezaad, S. Katiraci, A. Ghasemi, *Int J Adv Desg Manuf Tech.* **7(4)**, 1-6 (2014).
- [2]. M. Yousefpour, I. Vali, E. Saebnoori, *Int J Eng.* **27(10)**, 1627-1634 (2014)
- [3]. M. Kok, G. Ates, *Eur. Phys. J. Plus*, **132**, 185 (2017).
- [4]. M.L. Lethabena, P.A. Olubambi, H.K. Chikwanda, *J Mater Res Tech.* 1-10 (2015)
- [5]. M. Es-souni, M. Es-souni, H.F. Brandies, *Biometar.* **22**, 2153-2161 (2001)
- [6]. S.A.Thompson, *Int Endod J.* **33**, 297-310 (2000)
- [7]. D. Vojtech, J. Fojt, M. Voderova, P. Novak, L. Joska, *Metal, Czech Republic (Congress paper)* (2010)
- [8]. A. Bansiddhi, T.D. Sargeant, S.I. Stupp, D.C. Dunand, *Acta Biometar.* **4**: 773-782 (2008)
- [9]. A. Amini, C. Cheng, *Scientific Report.* **3(2476)** 1-6 (2013).
- [10]. C.H. Xu, X.Q. Ma, S.Q. Shi, C.H. Woo, *Mater Sci Eng: A.* **371(1)** 45-50 (2014).
- [11]. W. Ching, S.M. Abdus, *AIP Conference Proceedings.* **1901(1)** AIP Publishing (2017).
- [12]. A.W. Hansen, L.V.R. Beltrami, L.M. Antonini, D.J. Villarinho, J.C.K.D. Neves, C.E.B. Marino, C.D.F. Malfatti, *Mater Resch.* **18(5)** 1053-1061 (2015).
- [13]. M. Kok, K. Yildiz, *Appl Phy A Mater.* **116(4)** 2045-2050 (2014).

- [14]. C.H. Xu, S.Q. Shi, H.C. Man, C.H. Woo, C. Surya, *J Mater Sci.* **41(4:1)** 123-1129 (2006).
- [15]. G.S. Firstov, R.G. Vitchev, H. Kumar, B. Blanpain, J. Van Humbeeck, *Biomater.* **23(24)** 4863-4871 (2002).
- [16]. A.W. Hansen, L.V.R. Beltrami, L.M. Antonini, D.J. Villarinho, J.C.K.D. Neves, C.E.B. Marino, C.D.F. Malfatti, *Mater Resch.* **18(5)** 1053-1061 (2015).
- [17]. S.K. Sadrnezhaad, S.A. Hosseini, *Mater Design*, **30(10)** 4483-4487 (2009).
- [18]. H. Li, Y. Cong, Y. Zheng, L. Cui, *Mater Sci Eng C.* **60**, 554-559 (2016).
- [19]. M. Kok, G. Pirge, Y. Aydogdu, *Appl Surf Sci.* **268**, 136-140 (2013).
- [20]. S.H. El-Hadad, K.M. Ibrahim, L. Wagner, *Journal of Metallurgy*.1-6 (2014)
- [21]. A. Sami Abualnoun, K. Abdul Raheem, A. Abid, A.A. Murtadha, *Int J Mech Eng Tech (IJMET)*. **4(2)** 86-99 (2013)
- [22]. C.L. Chu, T. Hu, S.L. Wu, Y.S. Dong, L.H. Yin, P.H. Pu, C.Y. Lin, K.W.K. Chung, P.K. Yeung Chu, *Acta Biomater.* **3(5)**, 795-806 (2007).
- [23]. K.N. Lin, S.K. Wu, *Oxid Met.***71(3-4)**, 187-200 (2009).
- [24]. K.S. Kim, K.K. Jee, W.C. Kim, W.Y. Jang, S.H. Han, *Mater Sci Eng A*, **481**, 658-661 (2008).
- [25]. L. Zhang, C. Xie, J. Wu, *Mater Charac.* **58(5)** 471-478 (2007).
- [26]. K.S. Kim, K.K. Jee, Y.B. Kim, W.Y. Jang, S.H. Han, *The Eur Phys J Special Topics.* **158(1)** 67-71 (2008).
- [27]. A.S. Mahmud, C.W. Ng, M.F. Razali, *AIP Conference Proceedings.* **1774(1)**, 060006 (2016)